Journal of CO2 Utilization 93 (2025) 103038

Contents lists available at ScienceDirect

Journal of CO2 Utilization

journal homepage: www.elsevier.com/locate/jcou

Biogas upgrading through CO_2 methanation in a multiple-inlet fixed bed reactor: Simulated parametric analysis

P. Aragüés-Aldea, V.D. Mercader, P. Durán, E. Francés, J.Á. Peña, J. Herguido *

Catalysis and Reactor Engineering Group (CREG) - Aragon Institute of Engineering Research (I3A), Universidad de Zaragoza, c/ Mariano Esquillor s/n, Zaragoza 50018, Spain

ARTICLE INFO

Keywords:
Biogas upgrading
Distributed feeding
Methanation
Synthetic natural gas
Renewable hydrogen

ABSTRACT

A simulation of the catalytic CO_2 methanation reaction was carried out, evaluating the effect of reactants distributed feeding throughout the bed. The main operational parameters were studied in a multiple-inlet reactor to test their effect on conversions and, most importantly, on selectivities towards both CO and CH_4 as reaction products. The analyzed parameters were, firstly, the number of feeding points (*N*) and the dosage degree of reactants, followed by temperature (T), partial pressures of reactants (H_2:CO_2 ratios), and the composition of a sweetened biogas as feeding stream (CH_4:CO_2 ratios). It is confirmed that a distribution of biogas through several side inlets improves selectivities to the desired CH_4 product, over other feeding configurations. The effect of distributing reactants becomes intensified when the number of lateral feedings increases. This observation supports the experimental trends already proven in previous works. Regarding main operation parameters such as temperature and H_2:CO_2 molar ratio, the analysis confirmed that their influence on selectivities acts just as predicted at low conversions. However, when these conversions become higher the space velocity (WHSV) is the most important factor for selectivities. Finally, no significant changes in reaction performance were obtained when modifying the biogas CH_4:CO_2 ratio in the broad range of methane concentrations from 55 v% to 70 v%.

1. Introduction

In the last decades, energy-related and environmental issues have arisen as a problem that has to be addressed. While some options have already been suggested, such as use of renewable-based energy or advances in carbon capture, use and storage technologies (CCUS), none of them have been conclusively proven to be a definitive solution. More specifically, renewable-based energy is strongly dependent on uncontrollable conditions (i.e., the weather) and therefore cannot provide a stable supply.

In this context, the *Power-to-Gas* (PtG) strategy could play an essential role. This process is based on using surpluses of renewable electricity to split water molecules via electrolysis, generating hydrogen (H_2) that acts as an energy vector. Through a later methanation process, as described by the Sabatier reaction (r.1), it can be combined with carbon dioxide, generating a synthetic methane that can be injected into the natural gas grid or be stored for its later use during energy shortages [1]. When carbon dioxide comes from a biogas (mixture of CO_2 and CH_4 coming from the anaerobic decomposition of organic matter contained in some wastes), an additional benefit is obtained from the integration of these resources in the circular economy.

$$CO_2 + 4H_2 \rightleftharpoons CH_4 + 2H_2O \quad \Delta H^0_{Sabatier} 165.1 \left[kJ \cdot mol^{-1}\right] \qquad (r.1)$$

PtG technologies have received particular interest in recent years [2–4]. As this process has a high kinetic barrier, a catalyst is required in order to activate the molecules of carbon dioxide and hydrogen. Several solid catalysts might be used for this reaction, with Ni being the most used active species due to its high activity, selectivity, and low cost. Nevertheless, it tends to sinter, as well as shows relatively high selectivity for coke formation as drawbacks. This is particularly problematic when working at high temperatures (>500 °C) or low H_2:CO_2 ratios [5, 6]. Other active species include ruthenium, iron, cobalt and molybdenum, most of them being more active than nickel but less selective towards the *Sabatier* reaction (r.1) [7].

This reaction is exothermic and reversible, which results in the existence of a thermochemical limit that makes it unfavorable to work at high temperatures. On the other hand, kinetic limitations usually lead to poor performances at low temperatures, requiring the use of expensive materials as active catalytic phases [8]. As such, it is of great interest to

* Corresponding author.
E-mail address: jhergui@unizar.es (J. Herguido).

https://doi.org/10.1016/j.jcou.2025.103038
Received 13 December 2024; Received in revised form 30 January 2025; Accepted 4 February 2025
Available online 12 February 2025

improve this process, reaching optimal conditions to carry it out. An option includes use of multifunctional solids, which exploits the *Le Châtelier* principle, pushing reaction yields to go beyond thermochemical equilibrium predictions. Thus, very high performances can be reached, increasing yields from 10.6 % up to 85 % at relatively low temperatures of 275 °C [9]. This line of research can be divided into two aspects, one of them focusing on carbon dioxide capture [9,10], while the other is related to water adsorption, which intensifies the process by helping to achieve greater yields to methane and separating both products just after being generated [11]. This can be called *Sorption Enhanced Sabatier Reaction* (SESaR).

Another research field, also with the aim to optimize the methanation process, focuses on reactor design and configuration. By improving performances through different types of contact between the catalyst and reactants, an intensification of the process could be achieved. Traditionally, this reaction has been carried out on fixed bed reactors. However, the exothermicity of the *Sabatier* reaction (r.1) leads to the appearance of hot spots, which results in deactivation due to sintering, coke formation (with its subsequent fouling) and increase in selectivities towards nontarget products such as carbon monoxide.

For this reason, different types of reactors have been investigated [12,13]. Some of them are variations of a fixed bed, being either adiabatic or isothermal. The adiabatic variation usually has its temperature controlled by recirculating part of the product gas or dividing it into many stages while cooling the outlet [7]. It has nevertheless some disadvantages, such as low flexibility, high pressure drops, and the aforementioned existence of hot spots and increased selectivity towards undesired products. Meanwhile, isothermal reactors achieve a greater temperature control, as well as lower catalyst needs to reach a particular carbon dioxide conversion, but are more complex and expensive, in addition to the fact that a certain temperature gradient is unavoidable. In this sense, the option of working with configurations including several isothermal reactors (for example, two isothermal packed bed reactors operating in series at different temperatures with intermediate water removal) has recently been experimentally studied [8]. Fluidized bed reactors, on the other hand, are characteristically flexible, with a great heat transference that makes temperature nearly homogeneous. However, its drawback is that is complex to scale up, apart from low conversions and loss of solid as small particles (by attrition). Another option that has arisen is the use of structured reactors, which allows a good heat transference along with lower pressure drops.

In this frame, an additional possibility lies in distribution of feeding along the longitudinal direction of the reactor. This configuration has two advantages when carrying out carbon dioxide methanation; on one hand, controlling the introduction of one reactant helps confine the majority of the reaction to an area near the reactor inlet, thereby reducing the formation and intensity of hot spots and offering associated benefits. This approach was demonstrated many years ago with the lean distribution of oxygen in the oxidative coupling of methane (OCM) reaction [14]. Furthermore, as a two-stage process, contact type has a strong effect on selectivities towards products. This hypothesis in based on the consideration of *Sabatier* reaction as a series-parallel combination of two hydrogenation steps, based on the fact that the reaction mechanism results in the formation of two reaction products, undesired intermediate CO (carbon monoxide) through the reverse *Water Gas Shift – rWGS* (r.2), and methane as the final product in the reverse *Methane Steam Reforming* or *CO Methanation* (r.3) [6].

$$CO_2 + H_2 \rightleftharpoons CO + H_2O \quad \Delta H^0_{rWGS} = +41.2\,[\mathrm{kJ\ mol^{-1}}] \tag{r.2}$$

$$CO + 3H_2 \rightleftharpoons CH_4 + H_2O \quad \Delta H^0_{rSMR} = -206.3\,[\mathrm{kJ\ mol^{-1}}] \tag{r.3}$$

Two different types of reaction mechanisms have been proposed to explain how carbon dioxide methanation takes place. One of them includes an associative adsorption of both reactants, resulting in formation of intermediate species such as carbonyl and formate; the other path involves dissociation of carbon dioxide [15]. This one is the most widely accepted and explains generation of carbon monoxide as an intermediate product. When this mechanism is at work, lower conversions of carbon dioxide are related to a high selectivity towards carbon monoxide, evolving towards the opposite direction when space velocities decrease. This phenomenon was observed at low contact times by Larghi et al. [16], both with a nickel-based and a ruthenium-based catalyst –in the last case, selectivities towards CO rise up to 70 % at the greatest space velocity value with a 4 ^{wt}% Ru/Al_2O_3 catalyst, regardless of the tested temperature.

Chemical reactor engineering states that feeding carbon dioxide –which could be called the "*series*" reactant- through several side inlets leads to improved selectivities to the final product of the series reaction -methane-, over a conventional fixed bed reactor or one with distribution of the "*parallel*" reactant -hydrogen-, yielding this last greater selectivities towards carbon monoxide. This hypothesis has already been proven in previous papers [17,18], with a four-inlet reactor, both for carbon dioxide methanation and for biogas upgrading. Thus, for a given CO_2 conversion, side distribution of CO_2 yields the lowest selectivities towards CO of all three tested feeding configurations. These results could be considered for reactor design in a future scaling-up for building next generation of synthetic methane production plants.

The results shown in this paper aim to prove that the trends found experimentally are supported by theory, using for this an independent catalytic kinetics, obtained from bibliography [19–21]. In addition, this research is going to be extended, using a porous membrane to reach maximal distribution of the reactants so constituting a membrane wall packed bed reactor. Thus, it is of great interest to simulate the reaction performance of a multiple-inlet reactor, in order to predict how the results evolve when modifying the degree of side distribution of carbon dioxide or hydrogen. This simulation was carried out at different temperatures and space velocities, analyzing the effect of both parameters in carbon dioxide conversion and selectivity towards CO.

2. Experimental

2.1. Kinetics

To perform simulated reaction experiments in the proposed reactor configurations (i.e., with lateral feed distribution), a catalytic kinetics from the literature was chosen, corresponding to a Ni catalyst supported on zirconia (ZrO_2) [19]. Its composition had always a nickel/zirconium molar ratio (Ni/Zr) equal to 1. Kinetic equations for all three reactions -rWGS- (r.2), CO methanation -rSMR- (r.3), and direct CO_2 methanation -*Sabatier*- (r.1), were fitted to a *Langmuir-Hinshelwood-Hougen-Watson* (LHHW) model, specifically to the three-step one proposed by *Xu* and *Froment* [22]. They are presented as (Eqs. (1)–(3)). The values of their kinetic parameters are shown in the nomenclature chapter, at the end of this paper (Table 4). Kinetics constants are extracted from [19] and follow an *Arrhenius* type behaviour ($k_{r,0}$ and $E_{a,r}$ as in (Eq. (4))) while equilibrium constants are consistent with a *Van't Hoff* type ($K_{j,0}$ and ΔH_j as in (Eq. (5))) [20,21]. This applies for at all tested temperatures. No other products (i.e., other hydrocarbons or coke) were detected by analysis.

$$r_{Sab}\left(\frac{mol}{g\cdot s}\right) = \left[\frac{k_{Sab}\ .\ {P_{H2}}^{-7/2}.\left({P_{H2}}^{4}.P_{CO2} - \frac{{P_{H2O}}^{2}.P_{CH4}}{K_{eq,Sab}}\right)}{\left(1 + K_{CO}.P_{CO} + K_{H2}.P_{H2} + K_{CH4}.P_{CH4} + K_{H2O}.\frac{P_{H2O}}{P_{H2}}\right)^{2}}\right] \tag{1}$$

$$r_{rWGS}\left(\frac{mol}{g\cdot s}\right) = \left[\frac{k_{rWGS}\ .\ {P_{H2}}^{-1}.\left(P_{H2}.P_{CO2} - \frac{P_{CO}.P_{H2O}}{K_{eq,rWGS}}\right)}{\left(1 + K_{CO}.P_{CO} + K_{H2}.P_{H2} + K_{CH4}.P_{CH4} + K_{H2O}.\frac{P_{H2O}}{P_{H2}}\right)^{2}}\right] \tag{2}$$

$$r_{rSMR}\quad\left(\frac{mol}{g\,.\,s}\right)=\left[\frac{k_{rSMR}\quad.P_{H2}{}^{-5/2}\quad.\left(P_{H2}{}^{3}\,.P_{CO}-\frac{P_{H2O}\,.\,P_{CH4}}{K_{eq,rSMR}}\right)}{\left(1+K_{CO}\,.P_{CO}+K_{H2}\,.P_{H2}+K_{CH4}\,.P_{CH4}+K_{H2O}\,.\frac{P_{H2O}}{P_{H2}}\right)^{2}}\right] \tag{3}$$

$$k_r=k_{r,0}\,.\exp\left(\frac{-E_{a,r}}{R\,.\,T}\right)\quad\forall\quad r\in\{(r.1)\quad to\quad(r.3)\} \tag{4}$$

$$K_j\quad=\quad K_{j,0}\,.\exp\left(\frac{-\Delta H_j}{R\,.\,T}\right)\qquad\forall\quad j\in\{CO,\,H_2,\,CH_4,\,H_2O\} \tag{5}$$

$$K_{eq,Sab}\quad\left(MPa^{-2}\right)=\left(\frac{137}{0.101325}\right)^{2}\quad.\quad T^{3.998}\,.\exp\left(\frac{158.7}{R\,.\,T}\right) \tag{6}$$

$$K_{eq,rWGS}\quad(dimensionless)=\exp\left(4.33-\frac{4577.8}{T}\right) \tag{7}$$

$$K_{eq,rSMR}\quad\left(MPa^{-2}\right)=\quad\frac{K_{eq,Sab}}{K_{eq,rWGS}} \tag{8}$$

2.2. Reaction setup

For this simulation, an *ad-hoc* single dimension (axial) Plug Flow Reactor was built in *Matlab*® (R2023a), modifying one operating parameter at a time (the one taken as standard), while keeping the others constant. The analyzed parameters and operating conditions are shown in Table 1. Carbon dioxide conversions and selectivities towards carbon monoxide as undesired product, were calculated solving the system of ordinary differential equations (ODE) by means of a predictor-corrector based on an 8th order *Runge-Kutta* method (ODE89). The reactors were all supposed to adopt an isothermal regime and with negligible pressure drop. In addition, no diffusional constraints were considered during the reaction process.

The three main parameters analyzed in this work were the total number of inlets (*N*), temperature (T), and feed streams composition, both for hydrogen to carbon dioxide (H_2:CO_2) and methane to carbon dioxide (CH_4:CO_2) molar ratios. Since using multiple feeding points lead to dosing of the laterally fed reactant, and thus to a local defect of this substance, it is expected that an increase in the number of inlets will result in a greater degree of dosing, thereby intensifying the effect of each feeding configuration in the experimental results. In an extreme case, with a huge number of feeding points (*N* tending to infinity), it would result in a tubular reactor with a membrane as wall (i.e., a packed bed membrane reactor, PBMR). In this case, selectivities would deviate significantly from those obtained with a conventional fixed bed reactor. To give support to this concept, a parameter value of $N = 10{,}000$ inlets has been chosen as representative of a PBMR configuration, while $N = 1$ has been chosen as the one for a conventional FBR. In addition, intermediate options, such as $N = 4$ could be representative of a polytropic reactor (main plus three side feeds), identical to that used in previous studies of our research group [17,18]. All these configurations were included in the simulation test. All inlets were uniformly distributed throughout the reactor and the flow fed through each inlet was equal, simulating a uniformly distributed flow through the membrane pores in a future experimental work.

Table 1
Parameters and operating conditions.

	Standard value	Interval
Catalyst load, $W_{cat,0}$ (mg)	15.81	0.05–15,811.39
H_2:CO_2 molar ratio	4:1	1:1–7:1
CH_4:CO_2 molar ratio	7:3	11:9–7:3
Temperature set-point (°C)	400	250–400*
Total pressure (atm)	1	–
WHSV ((STP) mL g_{cat}^{-1} h^{-1})	$6.144{\cdot}10^{6}$	$6.144{\cdot}10^{3}$–$1.943{\cdot}10^{9}$
Total gas flow, q_0 ((STP) mL min^{-1})	1619.03	125–35,000
Number of inlets (*N*)	100	1–10,000

* at intervals of 25 °C (up to 7 temperatures).

Operating temperatures were also studied in a range from 250 to 400 °C. Reactions involved in the transformation of carbon dioxide into reaction products have different activation energies; consequently, temperatures do change reaction rates differently according to partial pressures at different positions within the catalyst bed, and might favour one reaction against others. This leads to significant changes in selectivities towards CH_4 or CO. Activation energy, as it was described in the kinetic mechanism of this catalyst [19], is lower for direct methanation (Sabatier, (r.1)) than for the two-staged path that involves carbon monoxide formation (rSMR, (r.2)) and its subsequent methanation (rWGS, (r.3)); as such, a lower temperature in this case should increase selectivities towards methane.

Lastly, partial pressures were modified to check their effect on reactor performances. The CO formation reaction (r.2) requires a smaller number of molecules than each of the methane generation ones (r.1) and (r.3); for this reason, operating in an excess of carbon dioxide may cause a rise in CO generation. In the situation where hydrogen is the reactant fed in excess, however, methane generation would be favoured over CO. In kinetic terms, this substantiates a lower order of dependence on hydrogen partial pressure for the reaction rate of reaction (r.2), than for reactions (r.1) and (r.3). Despite this and in practical terms, given that hydrogen production is usually the bottleneck of methane production, it is more advantageous to operate with lower partial pressures of this gas. Using the stoichiometric molar ratio (4:1) as a standard value, partial pressures of hydrogen and carbon dioxide were modified from 1:1 to 7:1.

In addition, the effect of raw biogas composition, strongly dependent on its origin and production conditions, must also be considered. This gaseous mixture contains impurities that might affect the performance of the plant, as is the case of hydrogen sulfide which poisons metal catalysts, or siloxanes that affect mechanical parts of process units like compressors. They must be removed prior to their entrance into the methanation process, giving rise to a sweetened biogas. Also, the relative contents of methane and carbon dioxide are susceptible to changes. As methane is a product of both, the reversible *Sabatier* reaction (r.1) and the reversible CO methanation (rSMR, (r.3)), its presence in the reaction environment as a component of the sweetened biogas might inhibit reactions and cause a reduction of conversions, as well as relatively favours the rWGS reaction (r.2). In kinetic terms, the order of detrimental dependence on the partial pressure of methane is greater for reactions (r.1) and (r.3) than for reaction (r.2). Should this be the case, it would be interesting to add previous separation stages, keeping a constant concentration of methane. Some alternatives include capturing carbon dioxide via pressure swing adsorption (PSA) [23], or separating selectively both compounds using membranes [24]. Although other impurities, like steam, nitrogen, oxygen, or the aforementioned hydrogen sulfide are always present, a sweetened biogas composition can be considered 55–70 v% of methane and 45–30 v% of carbon dioxide [25]. These two cases have been chosen as the extremes, while intermediate compositions will also be simulated to study their effect on yields towards carbon monoxide and methane.

Fig. 1A–C show the three feeding configurations adopted in this study. In the conventional fixed bed configuration (Fig. 1A), both reactants -H_2 and biogas- were fed simultaneously through a single inlet. Meanwhile, in the configurations with distributed feeding, labelled as polytropic (*Poly-*), one reactant was introduced through one inlet, located at the top of the reactor, while the other was distributed homogeneously (i.e., equal flowrates) and fed using all the side inlets (*N*). Thus, the configurations *Poly-H_2* (Fig. 1B), and *Poly-biogas* (Fig. 1C) were used when distributing hydrogen or biogas, respectively.

The simulation was carried out so that the molar flows of each substance were modified and calculated at each differential volume step along the longitudinal flow direction, by solving the corresponding mass

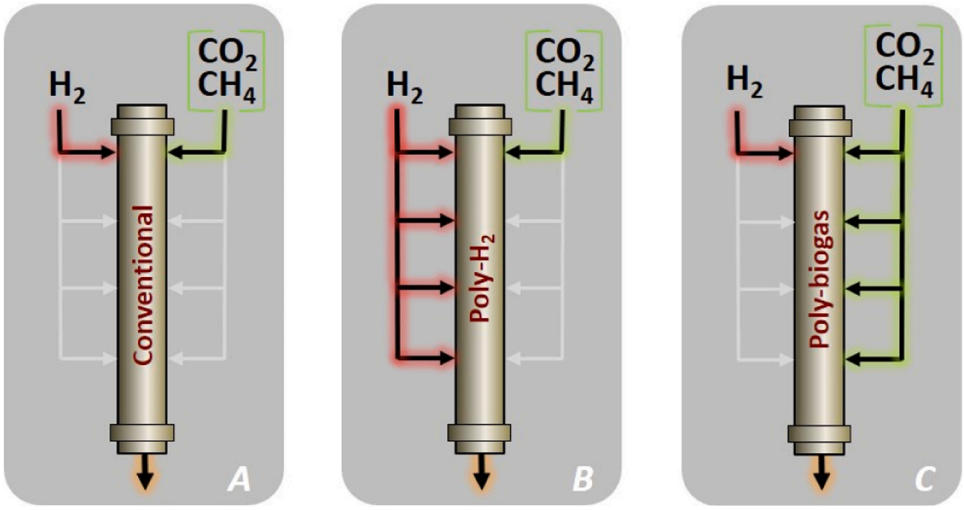

Fig. 1. Reactor sketches showing the outline of both reactants distribution in the catalytic packed bed reactor (PBR). $N = 4$. Feeding configurations: Conventional (A), *Poly-H_2* (B), and *Poly-biogas* (C).

balance (continuity equation) considering the adopted kinetic model of Section 2.1. Alongside them, to measure the configuration performances, were calculated the carbon dioxide conversion (Eq. (9)), hydrogen conversion (Eq. (10)), CO selectivity (Eq. (11)) and CH_4 selectivity (Eq. (12)).

$$CO_2\ conversion(\%) = \left[\frac{(f_{CO_2}|_{in} - f_{CO_2}|_{out})}{f_{CO_2}|_{in}}\right]\cdot 100 \tag{9}$$

$$H_2\ conversion(\%) = \left[\frac{(f_{H_2}|_{in} - f_{H_2}|_{out})}{f_{H_2}|_{in}}\right]\cdot 100 \tag{10}$$

$$CO\ selectivity(\%) = \left[\frac{f_{CO}|_{out}}{(f_{CO_2}|_{in} - f_{CO_2}|_{out})}\right]\cdot 100 \tag{11}$$

$$CH_4\ selectivity(\%) = \left[\frac{(f_{CH_4}|_{out} - f_{CH_4}|_{in})}{(f_{CO_2}|_{in} - f_{CO_2}|_{out})}\right]\cdot 100 \tag{12}$$

In these equations, $f_k|_{in}$ and $f_k|_{out}$ are total molar flows (mol·s^{-1}) of compound k entering or leaving the reactor, respectively. Since the only considered products were CO and CH_4, the addition of their selectivities must make one. Furthermore, conversions of both reactants are related between them and with selectivities to CO. These two relations (Eqs. (13) and (14)) were used to verify that the computer script was properly written. The constant C (Eq. (14)) is the fed molar ratio H_2:CO_2, (i.e., $C = f_{H_2}|_{in}/f_{CO_2}|_{in}$), which was varied as a study parameter.

$$CO\ \ selectivity\ (\%) = 100 - CH_4\ \ selectivity\ (\%) \tag{13}$$

$$\frac{H_2\ conversion\ (\%)}{CO_2\ conversion\ (\%)} = \frac{4}{C} - \frac{3}{C}\cdot\frac{CO\ selectivity\ (\%)}{100} \tag{14}$$

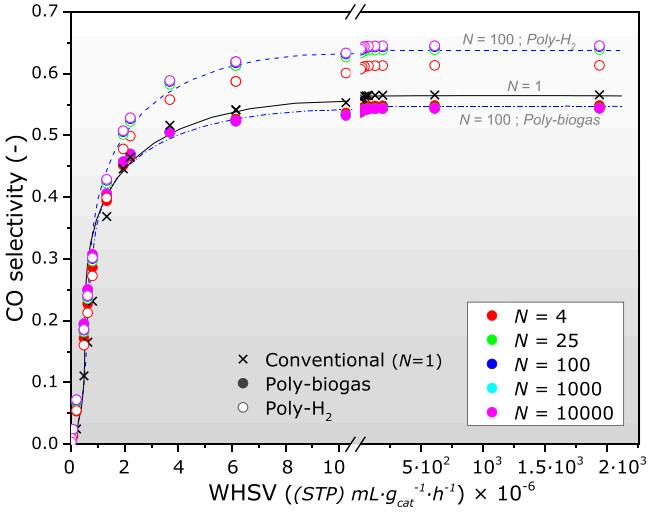

Fig. 2. Influence of side distribution in selectivities towards carbon monoxide, at different space velocities (*WHSV*) and number of side inlets (*N*). Molar ratio H_2:CH_4:CO_2 = 12:7:3. T = 400 °C. Dashed dotted lines for $N = 100$ feeding *Poly-biogas*; Dashed lines for $N = 100$ feeding *Poly-H_2*.

3. Results and discussion

3.1. Effect of the number of inlets (N)

The initial simulated experiments of this research were focused on determining the effect of varying the number of side inlets (*N*) of a fixed packed bed reactor (PBR). Thus, a study was made, both for conversions and selectivities towards carbon monoxide (as an undesired product) as a function of *N*. The values of this parameter were modified from 1 (a conventional fixed bed reactor) to 4 (corresponding to a polytropic fixed bed reactor PBR), 25, 100, 1000, and 10,000. In these studies, all flowrates were evenly distributed in space and equal between them, to

effectively simulate the differential amounts of gas passing through the porous membrane walls. Both reactants (CO_2 and H_2) were distributed, to analyze the effect on selectivities. The results do show that an increase in the number of lateral feeds for both reactants amplifies its influence on reaction performance, with selectivities either increasing along with *N* (for side distribution of H_2) or becoming lower when CO_2 dosing sites become greater (for side distribution of biogas). In addition, it was found that, for a high enough value of *N*, the effect on selectivities becomes less pronounced. This can be explained because, at greater number of side inlets, the '*Poly*' reactant is already very dosed, and thus its partial pressures are kept very low when compared to the other, 'conventionally' fed reactant. Fig. 2 depicts the achieved selectivities versus space velocities (*WHSV*) with different number of inlets (conventional or $N = 1$) and side distribution configurations (*poly-biogas* and *poly-H_2*).

Results in Fig. 2 show that, just as expected, side distribution of biogas leads to achieving lower selectivities to carbon monoxide than a conventional feeding of both reactants, or side distribution of H_2. This is in accordance with our initial hypothesis and research, and supports the advantages of this feeding configuration over the others, with cofeeding ($N = 1$) being an intermediate option and dosing of hydrogen (the '*attacking*' reactant) leading to a greater formation of CO. This effect, as already explained before, increases along with *N* value. This is because the dosed reactant's defect also becomes higher when the dosing degree is greater; thus, its partial pressures are kept low, favoring CH_4 (as seen in (r. 1) and (r. 3)) or CO formation (r. 2).

In addition, it was found that, while an increase in *N* will always result in an effect on selectivities, the differences become smaller when the reactants distribution is high enough, to the point of being almost equal at higher values of inlets (i.e., for the *poly-biogas* configuration, at the second greatest *WHSV* value tested, selectivities towards CO reach values of 54.36 % and 54.37 % for $N = 10{,}000$ and $N = 1000$, respectively). For this reason, it was decided to make a study of computation times (performed in an Intel Core2 Quad Q9550 @2.83 GHz), in order to find an optimal value of inlets to carry out this simulation. The computation times, as well as the results achieved in selectivities for both feeding configurations, are shown in Table 2.

As the data depicted in Table 2 demonstrate, and was previously shown in Fig. 2, it is confirmed that a higher degree of dosing eventually results in small differences of selectivity towards carbon monoxide. In fact, it has been observed that for the *poly-biogas* configuration, selectivities increase by less than 0.5 % when N exceeds 4. This suggests that once the number of inlets reaches a sufficient level, the effect of distribution becomes minimal, and there is no significant improvement in selectivity with further increases in *N*.

In addition, a higher value of *N* also requires a higher computational time, to the point that it exceeds 3 hours for $N = 10{,}000$. Thus, a trade-off number has been stablished at 100 inlets. When this value is used, the operational time is still low (slightly more than 2 minutes to obtain all conversions and selectivities required) while the results are very close to those achieved with 10,000 inlets (a difference of 0.03 % for the *poly-biogas* and 0.27 % for the *poly-H_2*). This value of the parameter *N* was then chosen as the standard, being used for the analysis of other parameters, namely the temperature and partial pressures of reactants. Furthermore, this side distribution with $N = 100$ can be considered high enough to be representative of how a packed bed reactor with a porous membrane wall (PBMR) would operate.

Table 2
Results of simulation for each value of *N* (number of inlets). T = 400 °C. *WHSV* = 6.144×10^8 (STP) mL g_{cat}^{-1} h^{-1}.

N	S_{CO} (*Poly-H_2*) (%)	S_{CO} (*Poly-biogas*) (%)	ΔS_{CO} (*Poly-H_2*) (%)	ΔS_{CO} (*Poly-biogas*) (%)	Computational time (min)
1	56.54	56.54	12.35	4.01	0.16
4	61.32	54.83	4.95	0.86	0.21
25	63.86	54.43	1.02	0.13	0.65
100	64.34	54.38	0.27	0.03	2.24
1,000	64.49	54.37	0.03	0.00	21.20
10,000	64.51	54.36	0.00	0.00	217.83

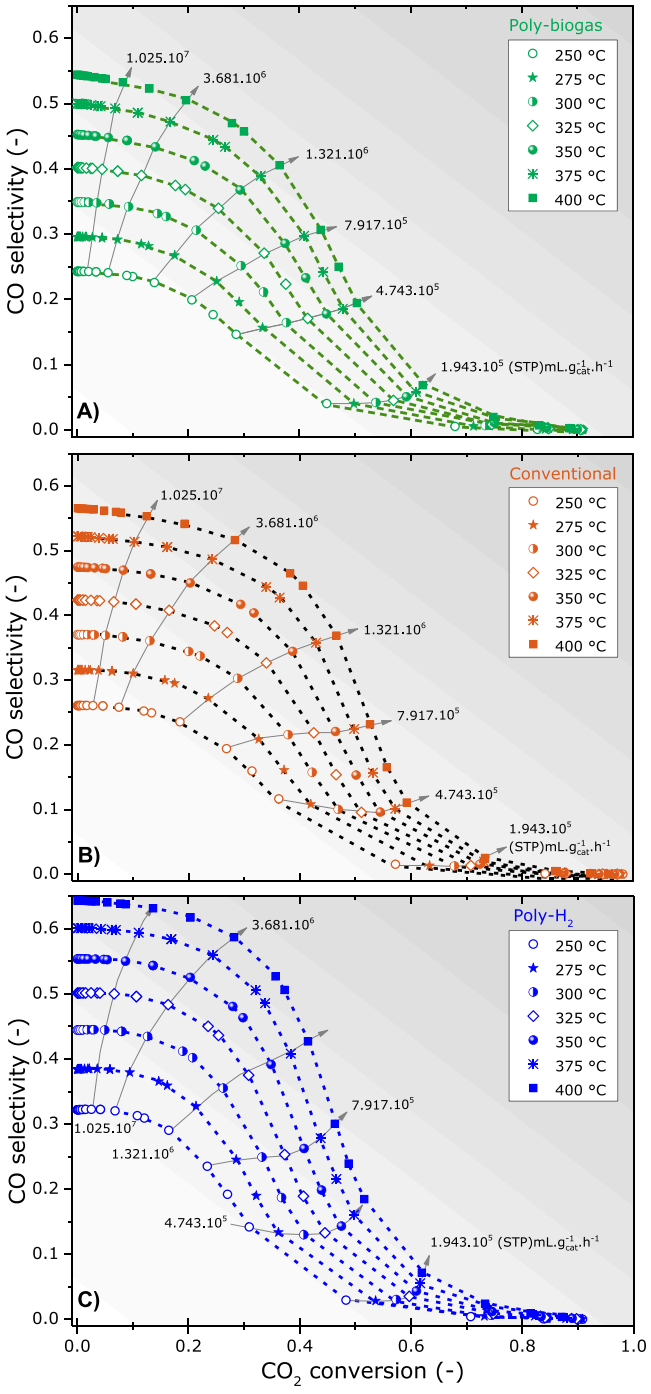

Fig. 3. Selectivities towards carbon monoxide vs. CO_2 conversion at different space velocities and temperatures. H_2:CH_4:CO_2 molar ratio = 12:7:3. Straight lines and figures: iso-space velocity (*WHSV* in (STP) mL g_{cat}^{-1} h^{-1}). Feeding configurations: A) *Poly-biogas*, B) conventional, C) *Poly-H_2*.

3.2. *Effect of temperature in reaction performance*

After choosing $N = 100$ as a representative value of the behavior of a PBMR with an acceptable computation time, it has been studied the influence of temperature in reaction performance. As the activation

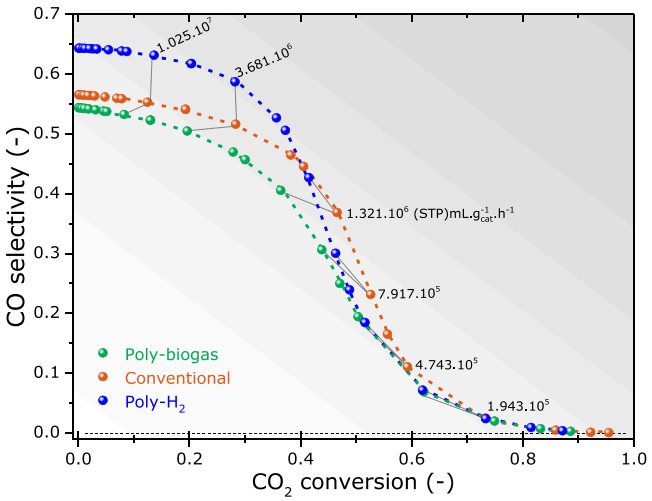

Fig. 4. Selectivities towards carbon monoxide vs. CO_2 conversion at different space velocities and feeding configurations. T = 400 °C. H_2:CH_4:CO_2 molar ratio = 12:7:3. Straight lines and figures: iso-space velocity (*WHSV* in (STP) mL g_{cat}^{-1} h^{-1}). Dashed lines: three different configurations attending their colours.

energy is lower for direct methanation (r. 1) over the path that involves CO formation and consumption (r. 2) and (r. 3), higher temperatures should favour greater selectivities towards CO [19]. As such, it would be more advantageous to work at a low temperature and space velocity, reaching higher selectivities towards methane at the same conversion. In Fig. 3 are represented conversions and selectivities for all three tested configurations (*Poly-biogas*, conventional, and *Poly-H_2*), at different temperatures (250–400 °C).

These results demonstrate that, for a given space velocity *WHSV*, working at a higher temperature results in greater conversions but also higher selectivities towards carbon monoxide. As explained before, this happens because activation energies are higher for the path that involves CO generation; thus, greater temperatures will always favour this mechanism over a direct methanation (r.1), which has no presence of this intermediate product. On the other hand, it is also proven that, for a specific conversion value and configuration, selectivities towards methane are at their highest at 250 °C and at their lowest at 400 °C, with the opposite trend taking place for selectivities to CO. This can be chalked up to *WHSV* being the dominant parameter over temperature in terms of selectivities. For a better visualization, in Fig. 3A (*Poly-biogas* configuration), at a fixed conversion value of 14 %, selectivities reach 22.59 % at 250 °C, 33.14 % at 300 °C, and 43.37 % at 350 °C. Although this study was carried out with a kinetic mechanism that favours CO formation at high temperatures, the same effect was observed with other kinetics that increase selectivities towards CH_4 along with temperature (as it is seen in Fig. 5B).

Fig. 4 shows the results obtained for a temperature of 400 °C comparing the three different configurations. Reactor feeding configuration was found to have a significant effect on the process results. Thus, as expected according to the previous experimental works of our group [17,18], dealing with distribution of biogas through the side inlets (*Poly-biogas*) results in greater selectivity towards methane than working with a conventional fixed bed, or one with side distribution of H_2 (*Poly-H_2*). However, it is necessary to mention that, with a conventional fixed bed reactor, higher conversions are generally achieved than with a reactor with distributed feed, regardless of whether it consists of H_2 or biogas (see lines of equal *WHSV* in Fig. 4).

In order to analyze the effect of the kinetic parameters of reactions

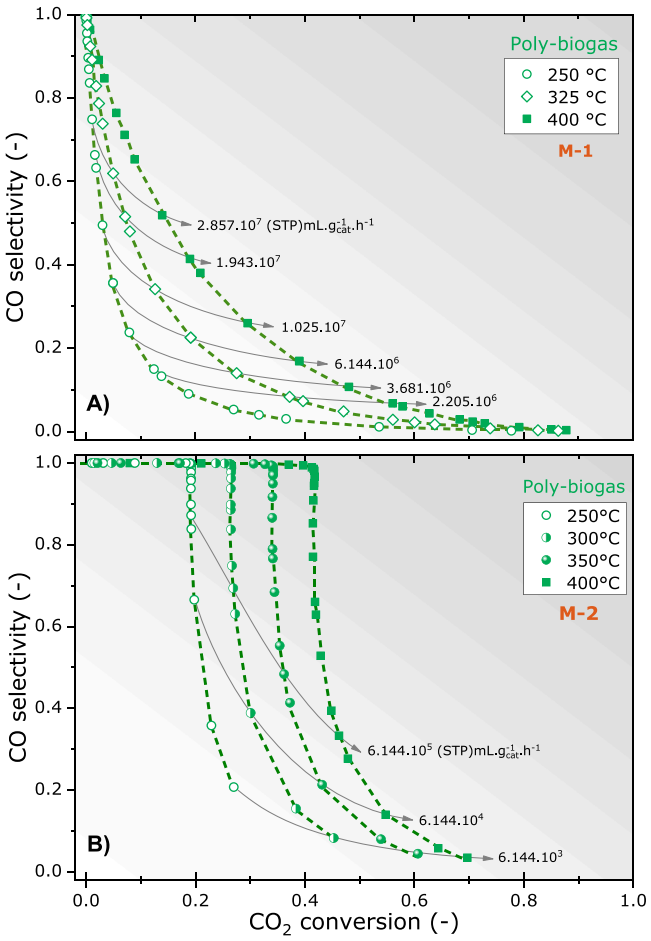

Fig. 5. Selectivities towards CO vs. CO_2 conversions for a *Poly-biogas* feeding configuration at different space velocities and temperatures. H_2:CH_4:CO_2 molar ratio = 12:7:3. Straight lines and figures: iso-space velocity (*WHSV* in (STP) mL g_{cat}^{-1} h^{-1}). Kinetic mechanism: A) M-1 ($k_{rWGS,0}$ = 4290 mol s^{-1} g_{cat}^{-1} MPa^{-1}; $k_{rSMR,0}$ = 418 mol s^{-1} g_{cat}^{-1} $MPa^{-1.5}$; Ea_{rWGS} = 50.9 kJ mol^{-1}; Ea_{rSMR} = 17.8 kJ mol^{-1}), B) M-2 ($k_{rWGS,0}$ = 418 mol s^{-1} g_{cat}^{-1} MPa^{-1}; $k_{rSMR,0}$ = 4290 mol s^{-1} g_{cat}^{-1} $MPa^{-1.5}$; Ea_{rWGS} = 17.8 kJ mol^{-1}; Ea_{rSMR} = 50.9 kJ mol^{-1}).

Table 3
Variations of the kinetic mechanism with respect to the base mechanism M-0.

Parameter	Units	Mechanism		
		M-0 (base)	**M-1** (Fig. 5A)	**M-2** (Fig. 5B)
$k_{Sab,0}$	mol s^{-1} g_{cat}^{-1} $MPa^{-1.5}$	151	-	-
$K_{rWGS,0}$	mol s^{-1} g_{cat}^{-1} MPa^{-1}	418	4290	418
$k_{rSMR,0}$	mol s^{-1} g_{cat}^{-1} $MPa^{-1.5}$	4290	418	4290
$E_{a,\ Sabatier}$	kJ mol^{-1}	17.8	-	-
$E_{a,\ rWGS}$	kJ mol^{-1}	43.3	50.9	17.8
$E_{a,\ rSMR}$	kJ mol^{-1}	50.9	17.8	50.9

(r.2) and (r.3) on the simulation results, Fig. 5 depicts selectivities and conversions achieved, using two different kinetic mechanisms. Both of them have as reference the base model (M-0) described by Choi et al. [19] but omitting direct methanation reaction (r.1). The first one (Fig. 5A), which is called M-1, adopts a greater activation energy for the first step (i.e., the rWGS reaction (r.2)) while the second one, M-2

(Fig. 5B) has the greatest activation energy for the second stage (i.e., the CO methanation, -rSMR- (r.3)). Table 3 shows the kinetic parameters considered for each mechanism.

Comparing the results for both kinetics (M-1 and M-2), it can be observed a similar qualitative behaviour of CO selectivity decrease with increasing CO_2 conversion. However, in the M-2 case there is a wide range of low conversions for which CO selectivity is complete, and this is wider when working at higher temperatures. For example, at 400 °C the selectivity to CO is total (100 %) for a conversion of 41.58 % (Fig. 5B). This coincides with the lower activation energy of the rWGS reaction generating CO in the M-2 kinetics. On the other hand, the results of this last analysis demonstrate that the parameter *WHSV* is the most influential for selectivities towards both products, regardless of reaction kinetics. Thus, even when working at a lower temperature favours CO production (both due to kinetics favouring higher selectivities and reaching lower conversions), decreasing operational flows or increasing the catalyst load would compensate this effect and minimize yields towards this undesired product. In this context, it would be more interesting to operate with a lower space velocity (or higher contact time) and temperature.

3.3. Partial pressures of reactants

The other parameters tested are partial pressures of reactants, both for hydrogen (i.e., the molar ratio H_2:CO_2) and methane (the molar ratio CH_4:CO_2, or biogas composition). Since the number of H_2 molecules that participate in CO generation (one) is different than that of methane formation (four), it is expected that working in defect of this reactant should increase selectivities towards CO, while an excess should favour CH_4 production. While this behaviour was indeed observed at low conversions, it changes when space velocities become lower and reaction performance intensifies. Fig. 6 shows the evolution of results when carrying out experiments at different partial pressures (1:1–7:1) and space velocities, for the three feeding configurations.

As these graphics demonstrate (Fig. 6), at low values of *WHSV* –which result in conversions becoming close to their maximum- selectivities towards CO decrease significantly, to the point of reaching almost zero values. This happens independently of the excess or defect of the reactants. On the other hand, when working at an excess of hydrogen, selectivities decrease more gradually at higher H_2:CO_2 ratios. These two trends confirm, as did the result obtained when analyzing the effect of temperatures, that space velocity eventually becomes the dominant parameter at low values. However, at low conversions the influence of partial pressures affects selectivities in the expected way –working in excess of H_2, which acts in both stages of the *Sabatier* reaction (r.1), favours methane production over carbon monoxide; the opposite happens when the carbon dioxide is the reactant fed in overstoichiometric ratios.

The last part of this work consisted of studying the effect of feeding CH_4:CO_2 molar ratio, or the composition of a sweetened biogas. Since biogas is a stream, obtained fundamentally from the anaerobic digestion of organic wastes, its composition might vary over time and overall depends on its origin and treatment. Therefore, it is necessary to consider it when working in the biogas upgrading process, as the presence of the methane could affect results and make necessary the use of previous stages of separation of carbon dioxide. Fig. 7 compares the different CH_4:CO_2 ratios (from 55 v% CH_4: 45 v% CO_2 to 70 v% CH_4: 30 v% CO_2) and the evolution of results for different *WHSV* values and for the three feeding configurations.

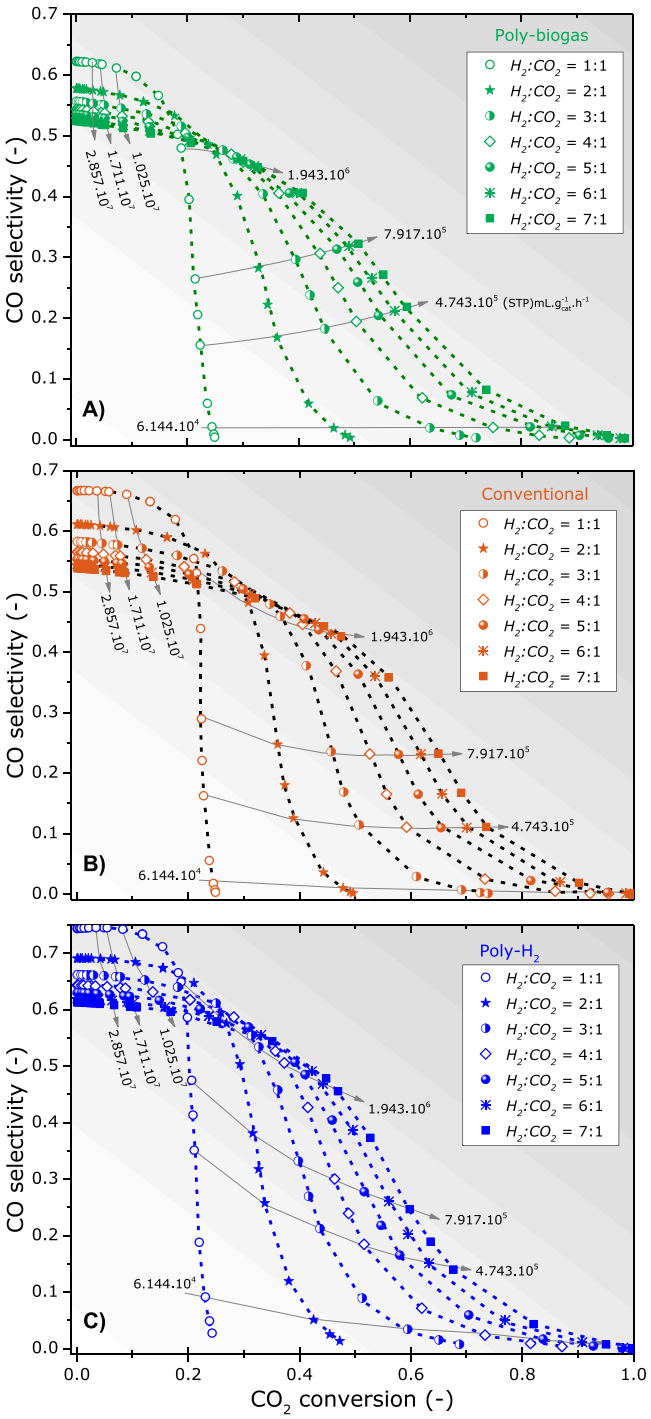

Fig. 6. Selectivities to CO vs. CO_2 conversions at different space velocities and H_2:CO_2 molar ratios. T = 400 °C. CH_4:CO_2 molar ratio = 7:3. Straight lines and figures: iso-space velocity (*WHSV* in (STP) mL g_{cat}^{-1} h^{-1}). Feeding configurations: A) *Poly-biogas*, B) conventional, C) *Poly-H_2*.

These last graphics reflect (Fig. 7) that there is, indeed, an effect of composition of the biogas in the reaction process. As the *Le Châtelier* principle states, the presence of different concentrations of methane

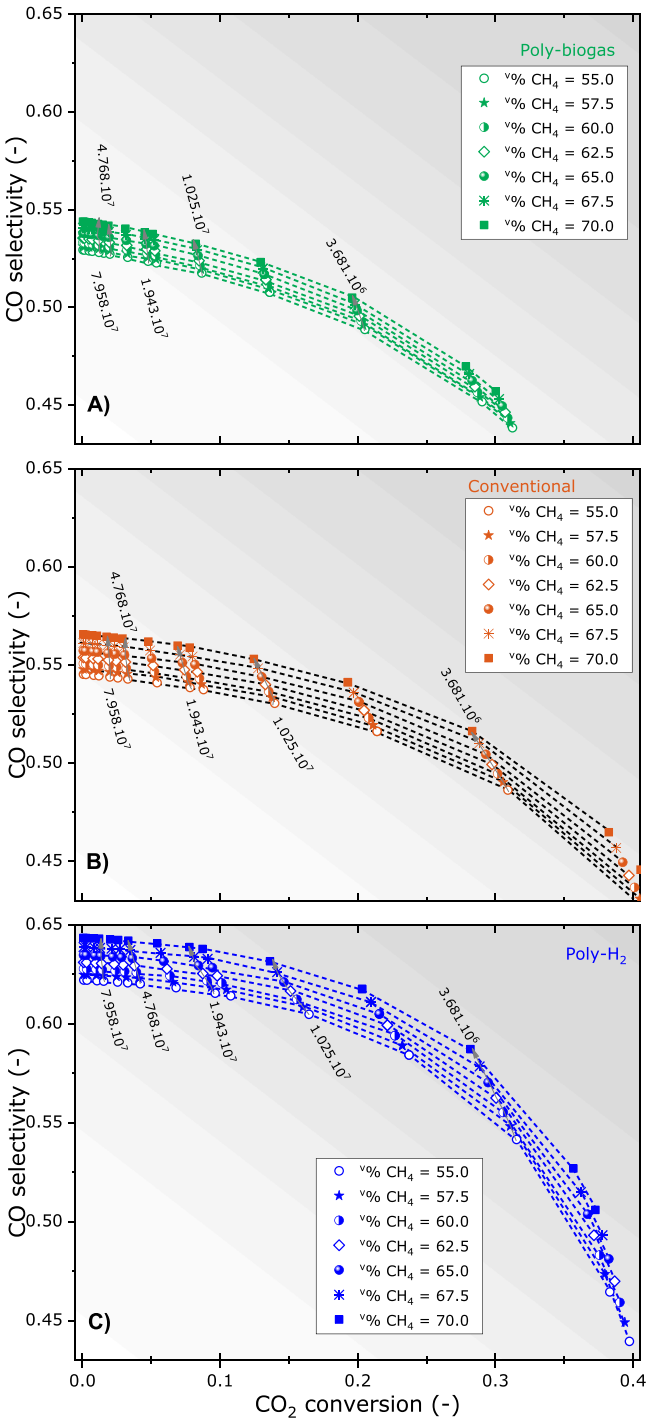

Fig. 7. Selectivities towards CO vs. CO_2 conversion at different space velocities and CH_4:CO_2 ratios. T = 400 °C. H_2:CO_2 = 4:1. Straight lines and figures: iso-space velocity (*WHSV* in (STP) mL g_{cat}^{-1} h^{-1}). Feeding configurations: A) *Poly-biogas*, B) conventional, C) *Poly-H_2*.

modifies conversions at iso-space velocity values, being lower at 70 v% CH_4. The same happens when looking at selectivities towards methane; they decrease when the biogas is more enriched in methane and become higher at lower methane concentrations. This is in accordance with the fact that, as reversible reactions, the presence of a product does eventually change the balance and favours the reverse reactions (i.e., the Steam Reforming of Methane –or *SMR*).

Nevertheless, it is also certain that the results are less different between compositions than it could be expected. Although conversions do change in a perceptible way, the variations are less than 5 % between the two extreme situations. Indeed, at a space velocity value of 3.68×10^6 (STP) mL g_{cat}^{-1} h^{-1}, conversions reach a value of 20.53 % with 55 % of methane (the lowest concentration value) and 19.60 % when working with 70 % (the highest). The same phenomenon is observed in selectivities. At the same space velocity, selectivities range from 48.86 % to 50.50 %, which accounts for slightly more than 3 % in relative terms.

These variations in results are sharper according to the tested feeding configuration. When hydrogen is the side distributed reactant (Fig. 7C), differences between conversions become wider (from 28.20 % to 31.54 %) as well as those of selectivities (from 54.16 % to 58.72 %); conventional feeding (Fig. 7B), on the other hand, becomes an intermediate condition, with the intervals of conversions going from 28.32 % to 30.92 %, and those of selectivities being 48.63 at their lowest and 51.63 % at their highest. However, since distribution of biogas is the most advantageous feeding configuration (Fig. 7A), this last factor should not be taken into account. It can be concluded, that although biogas composition does cause variations in results, these differences are not significant and it is unnecessary to add a separation stage that keeps a constant concentration of both methane and carbon dioxide.

4. Conclusions

The results in this work show a parametric study for the *Sabatier* reaction in the biogas upgrading process using a simulated, multiple-inlet fixed bed reactor. The first point of this research was studying the degree of side distribution of biogas and hydrogen through different numbers of inlets (*N*). It was concluded that dosing of biogas helps achieving higher selectivities towards methane than a conventional fixed bed or a side feeding of hydrogen. The influence of feeding configuration becomes more pronounced when the number of inlets increases, which marks a higher degree of distribution, clearly supporting the conclusions that were extracted from previous works [17, 18]. As such, a strong influence of contact between the reactants and catalyst has been detected, for all tested temperatures and space velocities (*WHSV*), and it highlights that the *Poly-biogas* configuration (or multiple side feeding of biogas) would bring improved yields to produce a Synthetic Natural Gas (SNG). Additionally, it is proven that selectivities to methane increase at a much slower rate after $N = 4$. This indicates that while there is always some improvement in results with an increasing number of inlets, the enhancements become less significant once the dosing level reaches a certain threshold.

Along the following analysis, an ideal number of 100 inlets was chosen (due to having reduced operational times and its results being very close to those obtained with higher values of this parameter). Simulations with this number of side feeding inlets ($N = 100$) could be considered representative of the behavior of a packed bed reactor with a

Table 4
Kinetic parameters (from Choi et al. [19]).

Parameter	Definition	Values	Units
ΔH_{CH4}	CH_4 adsorption enthalpy	−11.8	kJ mol^{-1}
ΔH_{CO}	CO adsorption enthalpy	19.4	kJ mol^{-1}
ΔH_{H2}	H_2 adsorption enthalpy	17.1	kJ mol^{-1}
ΔH_{H2O}	H_2O adsorption enthalpy	41.2	kJ mol^{-1}
$E_{a,Sab}$	Activation energy, for direct Sabatier reaction kinetic constant	17.8	kJ mol^{-1}
$E_{a,rSMR}$	Activation energy, for r-SMR reaction kinetic constant	50.9	kJ mol^{-1}
$E_{a,rWGS}$	Activation energy, for r-WGS reaction kinetic constant	43.3	kJ mol^{-1}
$K_{CH4,0}$	Pre-exponential factor, for CH_4 adsorption	1.04	MPa^{-1}
$K_{CO,0}$	Pre-exponential factor, for CO adsorption	3.07×10^{1}	MPa^{-1}
$K_{H2,0}$	Pre-exponential factor, for H_2 adsorption	7.35×10^{1}	MPa^{-1}
$K_{H2O,0}$	Pre-exponential factor, for H_2O adsorption	1.56×10^{3}	adim
$k_{Sab,0}$	Pre-exponential factor, for direct Sabatier reaction kinetic constant	1.51×10^{1}	mol s^{-1} g_{cat}^{-1} $MPa^{-1.5}$
$k_{rSMR,0}$	Pre-exponential factor, for r-SMR reaction kinetic constant	4.29×10^{3}	mol s^{-1} g_{cat}^{-1} $MPa^{-1.5}$
$k_{rWGS,0}$	Pre-exponential factor, for r-WGS reaction kinetic constant	4.18×10^{2}	mol s^{-1} g_{cat}^{-1} MPa^{-1}
R	Universal gas constant	8.314	J mol^{-1} K^{-1}

catalytic membrane wall (PBMR). Next parameters studied were temperatures and partial pressures, both for hydrogen (thus having excesses or defects of one of the reactants) and methane (for the simulation of different biogas compositions). In the case of temperatures and molar ratios H_2:CO_2, it was observed that selectivities towards desired methane increased when operating at a lower temperature (due to the chosen kinetic mechanism favouring CO formation at higher values) and at an excess of hydrogen. In any case, it was also observed that at a low enough value of *WHSV*, it becomes the most influential factor and that it overrides any effect of the two aforementioned conditions. This last observation was confirmed to take place when the kinetic mechanism favours methane formation at higher temperatures; thus, using a different catalyst would also yield the same conclusion. Additionally, when modifying partial pressures of hydrogen, selectivities did fall more sharply at a stronger defect of hydrogen and more gradually at an excess of this species. It is concluded, that a high contact time between the catalyst and the reaction mixture becomes the dominant parameter in selectivities towards the reaction products.

The last point of this paper deals with the composition of a biogas and the differences between conversions and selectivities achieved. In summary, it is observed that, although different results are achieved when the biogas varies its CH_4 content, conversions and selectivity values remain roughly similar, and it is not necessary to control its composition and keep a constant concentration in the feeding reaction mixture.

Nomenclature: Bibliography parameters

See Table 4

Declaration of Competing Interest

The authors declare that they have no known competing financial interests or personal relationships that could have appeared to influence the work reported in this paper.

Acknowledgements

This research has been funded by MICINN (Spanish Ministerio de Ciencia e Innovación) project number PID2022-136947OB-I00 and European Union Next Generation PRTR-C17.I1 Task LA4.A1. Additionally, the consolidated research group Catalysis and Reactor Engineering Group (CREG) (T43-23R) has received financial support from Gobierno de Aragón (Aragón, Spain) through the European Social Fund – FEDER. In addition, P. Aragüés-Aldea and V. D. Mercader express their gratitude for the research predoctoral grants of Gobierno de Aragón, in the first case, and Spanish Ministerio de Ciencia e Innovación (grant no. PRE2020-095679) in the latter. Lastly, authors also acknowledge the work of Servicio General de Apoyo a la Investigación-SAI (Universidad de Zaragoza).

Data availability

Data will be made available on request.

References

[1] R.R. Boggula, D. Fischer, R. Casaretto, J. Born, Methanation potential: suitable catalyst and optimized process conditions for upgrading biogas to reach gas grid requirements, Biomass Bioenergy 133 (2020) 105447, https://doi.org/10.1016/J.BIOMBIOE.2019.105447.
[2] G. Glenk, P. Holler, S. Reichelstein, Advances in power-to-gas technologies: cost and conversion efficiency, Energy Environ. Sci. 16 (12) (2023) 6058–6070, https://doi.org/10.1039/d3ee01208e.
[3] A. Maroufmashat, U. Mukherjee, M. Fowler, A. Elkamel, Power-to-gas: a new energy storage concept for integration of future energy systems, in: B. Mohammadi-Ivatloo Behnam, F. Jabari (Eds.), Operation, Planning, and Analysis of Energy Storage Systems in Smart Energy Hubs, Springer International Publishing, Cham, 2018, pp. 411–423, https://doi.org/10.1007/978-3-319-75097-2_17.
[4] CORDIS – European Comission, Power-to-gas system enables massive storage of renewable energy, 2020. ⟨http://doi.org/10.3030/717957⟩.
[5] J. Gao, Y. Wang, Y. Ping, D. Hu, G. Xu, F. Gu, F. Su, A thermodynamic analysis of methanation reactions of carbon oxides for the production of synthetic natural gas, RSC Adv. 2 (2015) 2358–2368, https://doi.org/10.1039/c2ra00632d.
[6] K. Stangeland, D. Kalai, H. Li, Z. Yu, CO_2 Methanation: the effect of catalysts and reaction conditions, Energy Procedia 105 (2017) 2022–2027, https://doi.org/10.1016/j.egypro.2017.03.577.
[7] S. Rönsch, J. Schneider, S. Matthiscke, M. Schlüter, M. Götz, J. Lefebvre, P. Prabhakaran, S. Bajohr, Review on methanation – from fundamentals to current projects, Fuel 166 (2015) 276–296, https://doi.org/10.1016/j.fuel.2015.10.111.
[8] A. Porta, C. Larghi, L. Lietti, C.G. Visconti, Once-through CO_2 hydrogenation to grid-compatible synthetic natural gas over a Ru-based catalyst at atmospheric pressure, Catal. Today 442 (2024) 114907, https://doi.org/10.1016/J.CATTOD.2024.114907.
[9] L. Gómez, I. Martínez, M.V. Navarro, R. Murillo, Selection and optimisation of a zeolite/catalyst mixture for sorption-enhanced CO_2 methanation (SEM) process, J. CO_2 Util. 77 (2023) 102611, https://doi.org/10.1016/J.JCOU.2023.102611.
[10] A. Bermejo-López, B. Pereda-Ayo, J.A. Onrubia-Calvo, J.A. González-Marcos, J. R. González-Velasco, Enhancement of the CO_2 adsorption and hydrogenation to CH_4 capacity of Ru–Na–Ca/γ–Al_2O_3 dual function material by controlling the Ru calcination atmosphere, J. Environ. Sci. 140 (2024) 292–305, https://doi.org/10.1016/J.JES.2023.08.041.
[11] M.S. Duyar, M.A.A. Treviño, R.J. Farrauto, Dual function materials for CO_2 capture and conversion using renewable H_2, Appl. Catal. B 168–169 (2015) 370–376, https://doi.org/10.1016/j.apcatb.2014.12.025.
[12] V.D. Mercader, P. Durán, P. Aragüés-Aldea, E. Francés, J. Herguido, J.Á. Peña, Biogas upgrading by intensified methanation (SESaR): reaction plus water adsorption - desorption cycles with Ni-Fe/Al_2O_3 catalyst and LTA 5A zeolite, Catal. Today 433 (2024) 114667, https://doi.org/10.1016/J.CATTOD.2024.114667.
[13] M. Tommasi, S.N. Degerli, G. Ramis, I. Rossetti, Advancements in CO_2 methanation: a comprehensive review of catalysis, reactor design and process optimization, Chem. Eng. Res. Des. 201 (2024) 457–482, https://doi.org/10.1016/J.CHERD.2023.11.060.
[14] J. Santamaría, M. Menéndez, J.Á. Peña, J.I. Barahona, Methane oxidative coupling in fixed bed catalytic reactors with a distributed oxygen feed. A simulation study,

Catal. Today 13 (2–3) (1992) 353–360, https://doi.org/10.1016/0920-5861(92)80160-O.

[15] B. Miao, S.S.K. Ma, X. Wang, H. Su, S.H. Chan, Catalysis mechanisms of CO_2 and CO methanation, Catal. Sci. Technol. 6 (12) (2016) 4048–4058, https://doi.org/10.1039/c6cy00478d.

[16] C. Larghi, A. Porta, R. Matarrese, C.G. Visconti, and L. Lietti, CO_2 methanation over Ru and Ni based catalysts: towards a comprehensive kinetic model through a multi-technique study, in: 15th European Congress on Catalysis (Europacat 2023), Prague - Czech Republic. August-September 2023. Book of abstracts, 2023. ⟨https://www.europacat2023.cz/Amca-Europacat2021/media/content/Docs/Book_of_abstracts-EuropaCat2023.pdf⟩.

[17] P. Aragüés-Aldea, A. Sanz-Martínez, P. Durán, E. Francés, J.Á. Peña, J. Herguido, Improving CO_2 methanation performance by distributed feeding in a Ni-Mn catalyst fixed bed reactor, Fuel 321 (2022) 124075, https://doi.org/10.1016/J.FUEL.2022.124075.

[18] P. Durán, P. Aragüés-Aldea, R. González-Pizarro, V.D. Mercader, F. Cazaña, E. Francés, J.Á. Peña, J. Herguido, Biogas upgrading through CO_2 methanation in a polytropic - distributed feed fixed bed reactor, Catal. Today 440 (2024) 114849, https://doi.org/10.1016/J.CATTOD.2024.114849.

[19] C. Choi, A. Khuenpetch, W. Zhang, S. Yasuda, Y. Lin, H. Machida, H. Takano, K. Izumiya, Y. Kawajiri, K. Norinaga, Determination of kinetic parameters for CO_2 methanation (Sabatier Reaction) over Ni/ZrO_2 at a stoichiometric feed-gas composition under elevated pressure, Energy Fuels 35 (24) (2021) 20216–20223, https://doi.org/10.1021/acs.energyfuels.1c01534.

[20] A. Quindimil, J.A. Onrubia-Calvo, A. Davó-Quiñonero, A. Bermejo-López, E. Bailón-García, B. Pereda-Ayo, D. Lozano-Castelló, J.A. González-Marcos, A. Bueno-López, J.R. González-Velasco, Intrinsic kinetics of CO_2 methanation on low-loaded Ni/Al_2O_3 catalyst: mechanism, model discrimination and parameter estimation, J. CO_2 Util. 57 (2022) 101888, https://doi.org/10.1016/J.JCOU.2022.101888.

[21] B. Smith R. J, M. Loganathan, M. Shekhar Shantha, A review of the water gas shift reaction kinetics, Int. J. Chem. React. Eng. 8 (1) (2010), https://doi.org/10.2202/1542-6580.2238.

[22] J. Xu, G.F. Froment, Methane steam reforming, methanation and water-gas shift: I. Intrinsic kinetics, AIChE J. 35 (1) (1989) 88–96, https://doi.org/10.1002/aic.690350109.

[23] A. Ali-Abd, M. Roslee-Othman, Z. Helwani, J. Kim, An overview of biogas upgrading via pressure swing adsorption: navigating through bibliometric insights towards a conceptual framework and future research pathways, Energy Convers. Manag. 306 (2024) 118268, https://doi.org/10.1016/J.ENCONMAN.2024.118268.

[24] A. Torre-Celeizábal, C. Casado-Coterillo, R. Abejón, A. Garea, Simultaneous production of high-quality CO_2 and CH_4 via multistage process using chitosan-based membranes, Sep. Purif. Technol. 320 (2023) 124050, https://doi.org/10.1016/J.SEPPUR.2023.124050.

[25] Q. Zhang, J. Hu, D.J. Lee, Biogas from anaerobic digestion processes: research updates, Renew. Energy 98 (2016) 108–119, https://doi.org/10.1016/J.RENENE.2016.02.029.